

## Charge Shift and Triplet State Formation in the 9-Mesityl-10-methylacridinium Cation

Andrew C. Benniston,<sup>†</sup> Anthony Harriman,<sup>\*,†</sup> Peiyi Li,<sup>†</sup> James P. Rostron,<sup>†</sup> Hendrik J. van Ramesdonk,<sup>‡</sup> Michiel M. Groeneveld,<sup>‡</sup> Hong Zhang,<sup>‡</sup> and Jan W. Verhoeven<sup>\*,‡</sup>

*Contribution from the Molecular Photonics Laboratory, School of Natural Science, University of Newcastle, Newcastle upon Tyne, NE1 7RU, United Kingdom, and Chemistry Department, HIMS, University of Amsterdam, Nieuwe Achtergracht 129, 1018 WS Amsterdam, The Netherlands*

Received May 6, 2005; E-mail: anthony.harriman@ncl.ac.uk

**Abstract:** The target donor–acceptor compound forms an acridinium-like, locally excited (LE) singlet state on illumination with blue or near-UV light. This LE state undergoes rapid charge transfer from the acridinium ion to the orthogonally sited mesityl group in polar solution. The resultant charge-transfer (CT) state fluoresces in modest yield and decays on the nanosecond time scale. The LE and CT states reside in thermal equilibrium at ambient temperature; decay of both states is weakly activated in fluid solution, but decay of the CT state is activationless in a glassy matrix. Analysis of the fluorescence spectrum allows precise location of the relevant energy levels. Intersystem crossing competes with radiative and nonradiative decay of the CT state such that an acridinium-like, locally excited triplet state is formed in both fluid solution and a glassy matrix. Phosphorescence spectra position the triplet energy well below that of the CT state. The triplet decays via first-order kinetics with a lifetime of ca. 30  $\mu$ s at room temperature in the absence of oxygen but survives for ca. 5 ms in an ethanol glass at 77 K. The quantum yield for formation of the LE triplet state is 0.38 but increases by a factor of 2.3-fold in the presence of iodomethane. The triplet reacts with molecular oxygen to produce singlet molecular oxygen in high quantum yield. In sharp contradiction to a recent literature report, there is no spectroscopic evidence to indicate the presence of an unusually long-lived CT state.

### Introduction

The formation of a long-lived charge-separated state is a prime requirement for artificial photosynthetic systems, optoelectronic devices, and photochemically driven machines.<sup>1</sup> An additional design feature inherent to all such molecular-scale materials is that, to offset fatigue, the electron-transfer processes should avoid diffusional motion. These realizations have led to the continued search for simple molecular systems in which rapid charge recombination is circumvented by competing secondary events.<sup>2</sup> In principle, the Marcus inverted effect<sup>3</sup> could be invoked to restrict the rate of charge recombination, while favoring fast charge separation, but complications from triplet formation,<sup>4</sup> quantum mechanical effects,<sup>5</sup> and nuclear tunneling<sup>6</sup> obscure the full impact of high reaction exoergonicity. As such, simple molecular dyads cannot be relied upon to display the

desired long-lived photoredox state.<sup>7</sup> The most satisfactory way around this problem has involved attaching additional electron donors and/or acceptors to the central dyad.<sup>8</sup> Such multicomponent supermolecules can initiate a cascade of electron-transfer steps leading to a spatially resolved radical pair.<sup>9</sup> Each electron-transfer event loses part of the initial excitation energy but, because of the incremental separation distance, stabilizes the

<sup>†</sup> University of Newcastle.

<sup>‡</sup> University of Amsterdam.

- (1) (a) Holten, D.; Bocian, D. F.; Lindsey, J. S. *Acc. Chem. Res.* **2002**, *35*, 57. (b) Shipway, A. N.; Willner, I. *Acc. Chem. Res.* **2001**, *34*, 421. (c) Wosnick, J. H.; Swager, T. M. *Curr. Opin. Chem. Biol.* **2000**, *4*, 715.
- (2) (a) Sanchez, L.; Perez, I.; Martin, N.; Guldi, D. M. *Chem. Eur. J.* **2003**, *6*, 2457. (b) Imahori, H. *Org. Biomol. Chem.* **2004**, *2*, 1425. (c) Park, Y. S.; Lee, E. J.; Chun, Y. S.; Yoon, Y. D.; Yoon, K. B. *J. Am. Chem. Soc.* **2002**, *124*, 7123. (d) Gust, D.; Moore, T. A.; Moore, A. L. *Acc. Chem. Res.* **2001**, *34*, 40. (e) Dürr, H.; Bossmann, S. *Acc. Chem. Res.* **2001**, *34*, 905.
- (3) Marcus, R. A. *Discuss. Faraday Soc.* **1960**, *29*, 21.

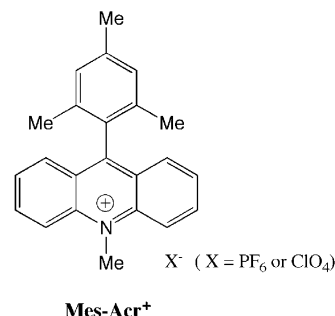
- (4) (a) Dutton, P. L.; Leigh, J. S.; Seibert, M. *Biochim. Biophys. Res. Comm.* **1972**, *46*, 406. (b) Thurnauer, M. C.; Katz, J. J.; Norris, J. R. *Proc. Natl. Acad. Sci. U.S.A.* **1975**, *72*, 3270. (c) Hasharoni, K.; Levanon, H.; Greenfield, S. R.; Gosztola, D. J.; Svec, W. A.; Wasielewski, M. R. *J. Am. Chem. Soc.* **1995**, *117*, 8055. (d) Wasielewski, M. R.; Minsek, D. W.; Niemczyk, M. P.; Svec, W. A.; Yang, N. C. *J. Am. Chem. Soc.* **1990**, *112*, 2823. (e) Brun, A. M.; Harriman, A.; Tsuboi, Y.; Okada, T.; Mataga, N. *J. Chem. Soc., Faraday Trans.* **1995**, *91*, 4047.
- (5) (a) Bixon, M.; Jortner, J. *Adv. Chem. Phys.* **1999**, *106*, 35. (b) Kroon, J.; Oevering, H.; Verhoeven, J. W.; Warman, J. M.; Oliver, A. M.; Paddon-Row, M. N. *J. Phys. Chem.* **1993**, *97*, 5065. (c) Smit, K. J.; Warman, J. M.; de Haas, M. P.; Paddon-Row, M. N.; Oliver, A. M. *Chem. Phys. Lett.* **1988**, *152*, 177. (d) Liang, N.; Miller, J. R.; Closs, G. L. *J. Am. Chem. Soc.* **1990**, *112*, 5353. (e) Warman, J. M.; Smit, K. J.; Jonker, S. A.; Verhoeven, J. W.; Oevering, H.; Kroon, J.; Paddon-Row, M. N.; Oliver, A. M. *Chem. Phys.* **1993**, *170*, 359.
- (6) (a) Kroon, J.; Oevering, H.; Verhoeven, J. W.; Warman, J. M.; Oliver, A. M.; Paddon-Row, M. N. *J. Phys. Chem.* **1993**, *97*, 5065. (b) Franzen, S.; Martin, J. *Annu. Rev. Phys. Chem.* **1995**, *46*, 453. (c) Benniston, A. C.; Chapman, G. M.; Harriman, A.; Mehrabi, M. *J. Phys. Chem. A* **2004**, *108*, 9026. (d) Ohkita, H.; Bente, H.; Anada, A.; Noguchi, H.; Kido, N.; Ito, S.; Yamamoto, M. *Phys. Chem. Chem. Phys.* **2004**, *6*, 3977.
- (7) (a) Verhoeven, J. W.; van Ramesdonk, H. J.; Groeneveld, M. M.; Benniston, A. C.; Harriman, A. *Chem. Phys. Chem.*, in press. (b) Verhoeven, J. W.; van Ramesdonk, H. J.; Zang, H.; Groeneveld, M. M.; Benniston, A. C.; Harriman, A. *Int. J. Photoenergy* **2005**, *7*, 103.

radical pair against charge recombination. In this way, despite the synthetic challenge, molecular triads, tetrads, pentads, etc. have become an essential part of our strategy to engineer intelligent molecular photonic devices.<sup>10</sup>

Apart from thermodynamic considerations, there are other possible ways to decrease the rate of charge recombination in simple molecular dyads.<sup>7</sup> For example, concepts based on spin restriction rules,<sup>11</sup> conformational gating,<sup>12</sup> applied magnetic fields,<sup>13</sup> orientational effects,<sup>14</sup> and orbital symmetry<sup>15</sup> have been considered as ways to avoid the time-consuming synthesis needed to produce the multicomponent arrays. The effects of these approaches tend to be limited and/or of restricted applicability.<sup>7</sup> A notable exception to this generic behavior, however, was reported recently. Thus, Fukuzumi et al.<sup>16</sup> described a donor–acceptor compound, namely the 9-mesityl-10-methylacridinium ion, that exhibits truly remarkable properties. This simple system is said to produce a photoredox state by way of a charge-shift reaction, in 98% yield, that survives for more than 2 h in benzonitrile at 203 K. The charge-transfer state is believed to store 2.37 eV and, because the reorganization energy for reforming the ground state is only 0.79 eV, classical Marcus theory predicts that the activation energy for this process is unusually high. Bimolecular charge shift is noted in aceto-

nitrile at ambient temperature, but this process becomes first order at higher temperatures and in frozen benzonitrile.<sup>16</sup> We have questioned these latter results<sup>17</sup> and suggested that the observed EPR signal might arise from a sacrificial photoredox process involving trace impurities in the solvent. Such behavior might also explain other results where long-lived photoredox products have been observed under unusual circumstances.<sup>18</sup>

The significance of the results reported by Fukuzumi et al.<sup>16</sup> cannot be overstated. In particular, the ability to stabilize a simple molecular dyad against charge recombination, nuclear tunneling, quantum mechanical effects, and triplet formation would open the way to construct all manner of fascinating optoelectronic devices without the need for elaborate synthesis. Already, this dyad has been proposed as an improved sensitizer for dye-injection solar cells,<sup>19</sup> as an olefin oxygenation photocatalyst,<sup>20</sup> and as a light harvester for photovoltaic cells.<sup>21</sup> Several questions have to be asked of the present system, however, before markedly changing strategy. A major issue concerns the lack of triplet formation since closely related 9-aryl-10-methylacridinium ions are known to exhibit efficient intersystem crossing to the triplet manifold.<sup>22</sup> Such donor–acceptor systems also display charge-transfer fluorescence<sup>22,23</sup> that decays on the nanosecond time scale. Of course, the mesityl group is held orthogonal to the acridinium nucleus, and this geometry might have profound implications for the extent of electronic coupling between the redox partners. It seems prudent, therefore, to conduct a detailed spectroscopic investigation of this system before drawing too many conclusions. We now describe the results of such an examination and find that although the 9-mesityl-10-methylacridinium cation displays some interesting photophysical properties these are very different from those reported by Fukuzumi et al.<sup>16</sup> and, in particular, do not include formation of a long-lived charge-transfer state.



## Experimental Section

All chemicals were purchased commercially and, unless stated otherwise, were used as received. Solvents for synthetic procedures were dried by standard literature methods before being distilled and stored under nitrogen over 4 Å molecular sieves. *N,N'*-Dimethyl-4,4'-

- (8) (a) Gust, D.; Moore, T. A.; Moore, A. L.; Macpherson, A. N.; Lopez, A.; DeGraziano, J. M.; Gouni, I.; Bittersman, E.; Seely, G. R.; Gao, F.; Nieman, R. A.; Ma, X. C.; Demanche, L.; Luttrell, D. K.; Lee, S. J.; Perrigan, P. K. *J. Am. Chem. Soc.* **1993**, *115*, 11141. (b) Imahori, H.; Guldí, D. M.; Tamaki, K.; Yoshida, Y.; Luo, C.; Sakata, Y.; Fukuzumi, S. *J. Am. Chem. Soc.* **2001**, *123*, 6617. (c) Kodis, G.; Liddell, P. A.; de la Garza, L.; Lin, S.; Moore, A. L.; Moore, T. A.; Gust, D. *J. Phys. Chem. A* **2002**, *106*, 2036. (d) Lukas, A. S.; Miller, S. E.; Wasielewski, M. R. *J. Phys. Chem. B* **2000**, *104*, 931. (e) Osuka, A.; Okada, T.; Taniguchi, S.; Nozaki, K.; Ohno, T.; Mataga, N. *Tetrahedron Lett.* **1995**, *36*, 5781. (f) Bell, T. D. M.; Jolliffe, K. A.; Ghigginio, K. P.; Oliver, A. M.; Shephard, M. J.; Langford, S. J.; Paddon-Row, M. N. *J. Am. Chem. Soc.* **2000**, *122*, 10661.
- (9) (a) Wasielewski, M. R. *Chem. Rev.* **1992**, *92*, 435. (b) Maruyama, K.; Osuka, A.; Mataga, N. *Pure Appl. Chem.* **1994**, *66*, 867. (c) Harriman, A.; Sauvage, J.-P. *Chem. Soc. Rev.* **1996**, *41*. (d) Sakata, Y.; Imahori, H.; Tsue, H.; Higashida, S.; Akiyama, T.; Yoshizawa, E.; Aoki, M.; Yamada, K.; Hagiwara, K.; Taniguchi, S.; Okada, T. *Pure Appl. Chem.* **1997**, *69*, 1951. (e) Gust, D.; Moore, T. A.; Moore, A. L. *Acc. Chem. Res.* **2001**, *34*, 40. (f) Paddon-Row, M. N. *Aust. J. Chem.* **2003**, *56*, 729.
- (10) (a) Linke, M.; Chambron, J.-C.; Heitz, V.; Sauvage, J.-P.; Encinas, S.; Barigelletti, F.; Flamigni, L. *J. Am. Chem. Soc.* **2000**, *122*, 11834. (b) Haycock, R. A.; Hunter, C. A.; James, D. A.; Michelsen, U.; Sutton, L. R. *Org. Lett.* **2000**, *2*, 2435. (c) Kim, Y. H.; Jeoung, D. H.; Kim, D.; Jeoung, S. C.; Cho, H. S.; Kim, S. K.; Aratani, N.; Osuka, A. *J. Am. Chem. Soc.* **2001**, *123*, 76. (d) Loewe, R. S.; Lammi, R. K.; Diers, J. R.; Kirmaier, C.; Bocian, D. F.; Holten, D.; Lindsey, J. S. *J. Mater. Chem.* **2002**, *12*, 1530.
- (11) (a) Smit, K. J.; Warman, J. M. *J. Lumin.* **1988**, *42*, 149. (b) Karpiuk, J. *Phys. Chem. Chem. Phys.* **2003**, *5*, 1078. (c) Anglos, D.; Bindra, V.; Kuki, A. *J. Chem. Soc., Chem. Commun.* **1994**, *2*, 213. (d) van Dijk, S. I.; Groen, C. P.; Hartl, F.; Brouwer, A. M.; Verhoeven, J. W. *J. Am. Chem. Soc.* **1996**, *118*, 8425. (e) Hviid, L.; Brouwer, A. M.; Paddon-Row, M. N.; Verhoeven, J. W. *Chem. Phys. Chem.* **2001**, *232*. (f) Hviid, L.; Bouwman, W. G.; Paddon-Row, M. N.; Verhoeven, J. W.; van Ramesdonk, H. J.; Brouwer, A. M. *Photochem. Photobiol. Sci.* **2003**, *2*, 995. (g) Hviid, L.; Verhoeven, J. W.; Brouwer, A. M.; Paddon-Row, M. N.; Yang, J.; George, M. W. *Photochem. Photobiol. Sci.* **2004**, *3*, 246.
- (12) (a) Osyczka, A.; Moser, C. C.; Daldal, F.; Dutton, P. L. *Nature* **2004**, *427*, 607. (b) Andreasson, J.; Kyrychenko, A.; Martensson, J.; Albinsson, B. *Photochem. Photobiol. Sci.* **2002**, *1*, 111. (c) Davis, W. B.; Ratner, M. A.; Wasielewski, M. R. *J. Am. Chem. Soc.* **2001**, *123*, 7877.
- (13) (a) Wolff, H.-J.; Burssner, D.; Steiner, U. E. *Pure Appl. Chem.* **1995**, *67*, 167. (b) Schaffner, E.; Fischer, H. *J. Phys. Chem.* **1996**, *100*, 1657. (c) Sinks, L. E.; Weiss, E. A.; Giaimo, J. M.; Wasielewski, M. R. *Chem. Phys. Lett.* **2005**, *404*, 244.
- (14) (a) Tsukahara, K.; Ueda, R. *Bull. Chem. Soc. Jpn.* **2003**, *76*, 561. (b) Korchowiec, J. *Int. J. Quantum Chem.* **2005**, *101*, 714. (c) Sakata, Y.; Imahori, H.; Tsue, H.; Higashida, S.; Akiyama, T.; Yoshizawa, E.; Aoki, M.; Yamada, K.; Hagiwara, K.; Taniguchi, S.; Okada, T. *Pure Appl. Chem.* **1997**, *69*, 1951. (d) Asano-Someda, M.; Jinmon, A.; Toyama, N.; Kaizu, Y. *Inorg. Chim. Acta* **2001**, *324*, 347.
- (15) (a) Zeng, Y.; Zimmt, M. B. *J. Am. Chem. Soc.* **1991**, *113*, 5107. (b) Zeng, Y.; Zimmt, M. B. *J. Phys. Chem.* **1992**, *96*, 8395. (c) Oliver, A. M.; Paddon-Row, M. N.; Kroon, J.; Verhoeven, J. W. *Chem. Phys. Lett.* **1992**, *191*, 371.
- (16) Fukuzumi, S.; Kotani, H.; Ohkubo, K.; Ogo, S.; Tkachenko, N. V.; Lemmetyinen, H. *J. Am. Chem. Soc.* **2004**, *126*, 1600.
- (17) Benniston, A. C.; Harriman, A.; Li, P.; Rostron, J. P.; Verhoeven, J. W. *Chem. Commun.* **2005**, 2701.
- (18) Guldí, D. M.; Imahori, H.; Tamaki, K.; Kashiwagi, Y.; Yamada, H.; Sakata, Y.; Fukuzumi, S. *J. Phys. Chem. A* **2004**, *108*, 541.
- (19) Hasobe, T.; Hattori, S.; Kamat, P. V.; Wada, Y.; Fukuzumi, S. *J. Mater. Chem.* **2005**, *15*, 372.
- (20) (a) Kotani, H.; Ohkubo, K.; Fukuzumi, S. *J. Am. Chem. Soc.* **2004**, *126*, 15999. (b) Ohkubo, K.; Nanjo, T.; Fukuzumi, S. *Org. Lett.* **2005**, *7*, 4265.
- (21) Hasobe, T.; Hattori, S.; Kotani, H.; Ohkubo, K.; Hosomizu, K.; Imahori, H.; Kamat, P. V.; Fukuzumi, S. *Org. Lett.* **2004**, *6*, 3103.
- (22) van Willigen, H.; Jones, G. I.; Farahat, M. S. *J. Phys. Chem.* **1996**, *100*, 3312.
- (23) Jones, G. I.; Farahat, M. S.; Greenfield, S. R.; Gosztola, D. J.; Wasielewski, M. R. *Chem. Phys. Lett.* **1994**, *229*, 40.

bipyridinium hexafluorophosphate (methyl viologen) was precipitated from an aqueous solution of the commercially available chloride salt by addition of  $\text{KPF}_6(\text{aq})$ . The resultant solid was filtered, washed thoroughly with water and  $\text{Et}_2\text{O}$ , and dried under vacuum. Recrystallization of the solid from  $\text{CH}_3\text{CN}/\text{Et}_2\text{O}$  afforded a pure white solid that was dried and kept over silica gel in a desiccator. 2,4,6-Triphenylpyrylium tetrafluoroborate (Aldrich Chemicals) was recrystallized several times from ethanol and dried under vacuum. Mesitylene was redistilled under vacuum. Benzonitrile was distilled under reduced pressure from  $\text{P}_2\text{O}_5$ , not  $\text{CaH}_2$ , since this latter drying agent leads to chemical decomposition.  $^1\text{H}$  (referenced to residual protiated solvent in  $\text{CD}_3\text{CN}$ ,  $\delta = 1.93$ ) and  $^{13}\text{C}$  NMR spectra were recorded with a JEOL Lambda 500 spectrometer. Routine mass spectra and elemental analyses were obtained using in-house facilities. Synthesis of *N*-(2-methoxyethoxymethyl)-9-acridone has been described previously.<sup>24</sup>

**Preparation of 9-Mesitylacridine.** To a solution of *N*-(2-methoxyethoxymethyl)-9-acridone<sup>24</sup> (1.0 g, 3.53 mmol) in tetrahydrofuran (THF) (100 mL) at 0 °C under nitrogen was added over 15 min a THF solution of 2-mesitylmagnesium bromide (freshly prepared from 2-bromomesitylene (1.2 mL, 7.76 mmol) in THF (30 mL) and magnesium turnings (0.22 g, 9.17 mmol)). The mixture was stirred at RT for 24 h and then heated at 50 °C for 12 h. A solution of concentrated HCl (50 mL) and  $\text{H}_2\text{O}$  (50 mL) was poured into the brown suspension. The resultant clear yellow solution was stirred overnight at RT. The mixture was treated with  $\text{K}_2\text{CO}_3(\text{aq})$  to give pH ca. 9 and extracted with ethyl acetate. The organic layer was washed with brine, separated, and dried over  $\text{MgSO}_4$ . Removal of the solvent afforded the crude product, which was purified by silica gel chromatography (petrol/ $\text{EtOAc}$  2:1) to give a pale-yellow crystalline solid (0.59 g, 56% yield).  $^1\text{H}$  NMR ( $\delta$ , 500 MHz,  $\text{CD}_3\text{CN}$ ): 1.65 (s, 6H,  $\text{CH}_3$ —), 2.42 (s, 3H,  $\text{CH}_3$ —), 7.15 (s, 2H, Ph—H), 7.45 (m, 4H, Acr—H), 7.80 (m, 2H, Acr—H), 8.21 (d,  $J = 8.8$  Hz, 2H, Acr—H).

**Preparation of 9-Mesityl-10-methylacridinium Hexafluorophosphate (Mes-Acr<sup>+</sup>).** To a solution of 9-mesitylacridine (0.24 g, 0.81 mmol) in  $\text{CH}_3\text{CN}$  (20 mL) was added  $\text{CH}_3\text{I}$  (0.35 mL, 5.56 mmol). The mixture was refluxed overnight. The volume of the mixture was reduced to ca. 2 mL, and 100 mL of ether was added. The resultant brown-red solid (0.15 g) was collected by filtration and washed with diethyl ether. The solid was dissolved in a mixture of  $\text{CH}_3\text{CN}$  (20 mL)/ $\text{H}_2\text{O}$  (10 mL), and  $\text{KPF}_6$  (0.70 g, 3.80 mmol) in  $\text{H}_2\text{O}$  (20 mL) added to afford a light-yellow crystalline solid that was collected by filtration and washed with  $\text{H}_2\text{O}$  and diethyl ether. Bright yellow crystals were obtained by recrystallization from  $\text{CH}_3\text{OH}$  and diethyl ether. Yield: 0.15 g (41%).  $^1\text{H}$  NMR ( $\delta$ , 500 MHz,  $\text{CD}_3\text{CN}$ ): 1.68 (s, 6H,  $\text{CH}_3$ —), 2.46 (s, 3H,  $\text{CH}_3$ —), 4.82 (s, 3H,  $\text{CH}_3$ —N), 7.23 (s, 2H, Ph—H), 7.84 (d,  $J = 5$  Hz), 4H, Acr—H), 8.38 (m, 2H, Acr—H), 8.61 (d,  $J = 9.3$  Hz, 2H, Acr—H). ES-MS ( $m/z$ ): 312.1 (calcd  $M_r = 312.2$  for  $[\text{M} - \text{PF}_6]^+$ ). Anal. Calcd for  $\text{C}_{23}\text{H}_{22}\text{NPF}_6$ : C, 60.40; H, 4.85; N, 3.06%. Found: C, 60.40; H, 4.65; N, 3.17%.

**Preparation of 9-Mesityl-10-methylacridinium Perchlorate.** 9-Mesityl-10-methylacridinium iodide (60 mg, 0.137 mmol) was dissolved in a mixture of  $\text{CH}_3\text{CN}$  (2 mL) and  $\text{H}_2\text{O}$  (20 mL). To this yellow solution was added  $\text{NaClO}_4$  (0.10 g) in  $\text{H}_2\text{O}$  (20 mL). The resulting light orange-yellow precipitate was collected by filtration and washed with  $\text{H}_2\text{O}$  and ether. Orange crystals were obtained by recrystallization from  $\text{CH}_3\text{OH}/\text{CH}_3\text{CN}$  and ether.<sup>25</sup> The authenticity of this sample was confirmed by a single-crystal X-ray diffraction study (see the Supporting Information). Yield: 50 mg (89%).  $^1\text{H}$  NMR ( $\delta$ , 500 MHz,  $\text{CD}_3\text{CN}$ ): 1.68 (s, 6H,  $\text{CH}_3$ —), 2.46 (s, 3H,  $\text{CH}_3$ —), 4.81 (s, 3H,  $\text{CH}_3$ —N), 7.23

(s, 2H, Ph—H), 7.84 (d,  $J = 5$  Hz, 4H, Acr—H), 8.37 (m, 2H, Acr—H), 8.60 (d,  $J = 9.3$  Hz, 2H, Acr—H). ES-MS ( $m/z$ ): 312.2 (calcd  $M_r = 312.2$  for  $[\text{M} - \text{ClO}_4]^+$ ). Anal. Calcd for  $\text{C}_{23}\text{H}_{22}\text{NClO}_4$ : C, 67.07; H, 5.38; N, 3.40%. Found: C, 67.07; H, 5.42; N, 3.42%. *Note that the possible shock sensitivity of organic perchlorates requires that these are handled carefully and in small quantities only.*

Photophysical studies were made in parallel in both Amsterdam and Newcastle with fully consistent results. Absorption spectra were recorded with a Hitachi U3310 spectrophotometer, and luminescence spectra were recorded with a fully corrected Yvon-Jobin Fluorolog tau-3 spectrophotometer. Emission spectra were recorded for optically dilute solutions after purging with  $\text{N}_2$ . Spectral curve fitting was carried out as described before.<sup>26</sup> The spectrum was fully corrected, reduced,<sup>27</sup> and deconvoluted into Gaussian components<sup>28</sup> using the commercially available software PEAKFIT. Luminescence quantum yields were determined relative to that of 9-phenyl-10-methylacridinium chloride in acetonitrile.<sup>22</sup> Temperature dependence studies were made with sealed sample cells housed in an Oxford Instruments Optistat DN cryostat. Emission lifetimes were measured at room temperature with the tau-3 spectrophotometer. For lower temperatures, the luminescence lifetimes were measured by time-correlated, single-photon counting using a high repetition (40 MHz) picosecond laser diode operating at 440 nm. Emission was isolated from scattered laser light with a high-radiance monochromator and detected with a microchannel plate photocell. After deconvolution of the instrument response function, the time resolution of this setup was ca. 15 ps. The spectral resolution, being limited by the need to obtain a reasonable count rate, was ca. 4 nm. Improved time resolution was achieved using fluorescence upconversion methods as described previously.<sup>29</sup>

Flash photolysis studies were made with a variety of instruments. An Applied Photophysics Ltd. LKS60 was used for nanosecond studies. Excitation was made with 4-ns pulses at 355 nm delivered with a frequency-tripled, Q-switched Nd:YAG laser, while detection was made at 90° using a pulsed, high-intensity Xe arc lamp. The signal was detected with a fast response PMT after passage through a high-radiance monochromator. Transient differential absorption spectra were recorded point-by-point with 5 individual records being averaged at each wavelength. Kinetic measurements were made after averaging 50 individual records using global analysis methods. The sample was purged with  $\text{N}_2$  before use. For some studies, iodomethane (10% v/v) was added before photolysis. The laser intensity was calibrated by reference to the triplet state of benzophenone in deoxygenated acetonitrile.<sup>30</sup> Quantum yield measurements were made by reference to benzophenone in acetonitrile over a wide range of laser intensities. For these studies, the triplet quantum yield and  $T_1 - T_n$  molar absorption coefficient at 525 nm for benzophenone were taken as 1.0 and 6500  $\text{M}^{-1} \text{cm}^{-1}$ , respectively.<sup>31</sup> The molar absorption coefficient for Mes-Acr<sup>+</sup> at 500 nm was measured by the complete conversion method to be 5500  $\text{M}^{-1} \text{cm}^{-1}$ ; this latter value is in excellent agreement with that determined for the conjugate acid of acridine.<sup>32</sup> For the complete bleaching studies, the excitation source was a pulsed Xe flash lamp (fwhm <1  $\mu\text{s}$ ) and the optical cell was a 10 cm path length glass cylinder. The solution was deoxygenated by freeze—pump—thaw cycles, and the flash lamp was filtered to remove UV ( $\lambda < 330$  nm) light.

(24) Tanaka, T.; Tasaki, T.; Aoyama, Y. *J. Am. Chem. Soc.* **2002**, *124*, 12454.

(25) The  $^1\text{H}$  NMR spectrum recorded for the perchlorate salt differs from that reported in the literature (ref 20a). This is not due to ion pairing since our spectra for perchlorate and hexafluorophosphate samples are indistinguishable. Furthermore, we note that all the chemical shifts differ by ca. 0.5 ppm (ref 20) and this effect is most likely caused by incorrect referencing to the residual protiated solvent peak. Closely comparable spectra were found in  $\text{CDCl}_3$  and between the two laboratories.

(26) (a) Bixon, M.; Jortner, J.; Verhoeven, J. W. *J. Am. Chem. Soc.* **1994**, *116*, 7349. (b) Gould, I. R.; Young, R. H.; Mueller, L. J.; Albrechts, A. C.; Farid, S. *J. Am. Chem. Soc.* **1994**, *116*, 8188. (c) Bixon, M.; Jortner, J.; Cortés, J.; Heitele, H.; Michel-Beyerle, M. E. *J. Phys. Chem.* **1994**, *98*, 7289. (d) Oevering, H.; Verhoeven, J. W.; Paddon-Row, M. N.; Warman, J. M. *Tetrahedron* **1989**, *45*, 4751. (e) Cortés, J.; Heitele, H.; Jortner, J. *J. Phys. Chem.* **1994**, *98*, 2527.

(27) Parker, C. A.; Rees, W. T. *Analyst* **1960**, *85*, 587.

(28) Harriman, A.; Hissler, M.; Ziessel, R. *Phys. Chem. Chem. Phys.* **1999**, *1*, 4203.

(29) Harriman, A.; Hissler, M.; Trompette, O.; Ziessel, R. *J. Am. Chem. Soc.* **1999**, *121*, 2516.

(30) Carmichael, I.; Hug, G. L. *J. Phys. Chem. Ref. Data* **1986**, *15*, 1.

(31) Bensasson, R. V.; Gramain, J.-C. *J. Chem. Soc., Faraday Trans. 1* **1980**, *76*, 1801.

(32) Nishida, Y.; Kikuchi, K.; Kokubun, H. *J. Photochem.* **1980**, *13*, 75.



Improved time resolution was achieved with a mode-locked, frequency-doubled Nd:YAG laser (fwhm = 20 ps). The excitation pulse was passed through a Raman shifter in order to isolate the required wavelength. The monitoring pulse was either a white light continuum, delayed with respect to the excitation pulse with a computer-controlled optical delay line, or a pulsed Xe arc lamp. For the former studies, the two pulses were directed almost collinearly through the sample cell. The monitoring pulse was dispersed with a Princeton Instruments spectrograph and detected with a dual-diode array spectrometer. Approximately 150 individual laser shots were averaged at each delay time. Kinetic parameters were derived by overlaying spectra collected at different delay times. All measurements were made with dilute solutions after purging with N<sub>2</sub>. For the latter studies, a fast response digitizer and PMT were used as detector at a single wavelength. The temporal resolution of this setup was about 2 ns.

Fast transient spectroscopy was made by pump–probe techniques using femtosecond pulses delivered from a Ti:sapphire generator amplified with a multipass amplifier pumped via the second harmonic of a Q-switched Nd:YAG laser. The amplified pulse energies varied from 0.3 to 0.5 mJ, and the repetition rate was kept at 10 Hz. Part of the beam (ca. 20%) was focused onto a second-harmonic generator in order to produce the excitation pulse. The residual output was directed onto a 4-mm sapphire plate so as to create a white light continuum for detection purposes. The continuum was collimated and split into two equal beams. The first beam was used as reference, while the second beam was combined with the excitation pulse and used as the diagnostic beam. The two beams were directed to different parts of the entrance slit of a cooled CCD detector and used to calculate differential absorbance values. The CCD shutter was kept open for 1 s, and the accumulated spectra were averaged. This procedure was repeated until about 100 individual spectra had been averaged. Time-resolved spectra were recorded with a delay line stepped in increments of 100 fs for short time measurements. This step length was increased for longer time measurements. The decay profiles were fitted globally as the sum of exponentials and deconvoluted with a Gaussian excitation pulse. The group velocity dispersion across one spectrum (ca. 220 nm) was of the order of 1 ps, and the overall temporal resolution of this setup was ca. 0.8 ps. The sample, possessing an absorbance of ca. 1 at 430 nm, was flowed through a quartz cuvette (optical path length = 1 mm) and maintained under an atmosphere of N<sub>2</sub>.

Singlet molecular oxygen was detected by time-resolved luminescence after excitation of the sample in O<sub>2</sub>-saturated acetonitrile with a 10-ns laser pulse delivered at 355 nm. The detector was a cryogenically cooled Ge photocell operating at 1270 nm. The laser intensity was varied over a wide range using metal screen filters and, in each case, 20 separate laser shots were averaged to produce the final signal. The yield of singlet molecular oxygen was obtained by extrapolation of the first-order decay trace to zero time. An optically matched solution of perinaphthenone in O<sub>2</sub>-saturated acetonitrile was used as reference.<sup>33</sup>

The transient differential absorption spectrum of the mesityl  $\pi$ -radical cation was recorded by laser flash photolysis ( $\lambda = 355$  nm, fwhm = 4 ns) of 2,4,6-triphenylpyrylium tetrafluoroborate (TPP<sup>+</sup>) ( $2.5 \times 10^{-5}$  M) in air-equilibrated acetonitrile containing mesitylene (0–0.1 M).<sup>34</sup> At the end of the laser pulse, the transient differential absorption spectrum comprises ground-state bleaching, triplet TPP<sup>+</sup> ( $\lambda_{\text{MAX}} = 340$  and 470 nm), TPP<sup>•</sup> ( $\lambda_{\text{MAX}} = 550$  nm), and the mesityl  $\pi$ -radical cation. The triplet lifetime is unaffected by the presence of mesitylene, but pronounced fluorescence quenching occurs. The lifetime of the triplet state, being set by the concentration of dissolved O<sub>2</sub>, was ca. 1  $\mu$ s.

After decay of the triplet state,<sup>34a</sup> the residual spectrum contains contributions from the neutral TPP<sup>•</sup> radical<sup>34b</sup> and the mesityl  $\pi$ -radical cation.<sup>34c,d</sup> Global analysis of the kinetic data and subtracting the former spectrum ( $\epsilon_{550} = 2790 \text{ M}^{-1} \text{ cm}^{-1}$ ) provides access to the absorption spectrum of the mesityl  $\pi$ -radical cation. Confirmation of this latter assignment was made by addition of low concentrations of 4,4'-dimethoxydiphenylmethanol, which was oxidized by the mesityl  $\pi$ -radical cation to form the known spectrum ( $\lambda_{\text{MAX}} = 510$  nm) of the 4,4'-dimethoxydiphenylmethyl cation.<sup>34e</sup>

Electrochemical measurements were made with an HCH electrochemical analyzer. The working electrode was a highly polished glassy carbon disk, and the counter electrode was a Pt wire. A Ag/AgCl reference electrode was used, with ferrocene as internal standard. The solution (ca. 1 mM) contained tetra-*N*-butylammonium hexafluorophosphate (0.2 M) as background electrolyte and was purged thoroughly with N<sub>2</sub> prior to electrolysis. Peak potentials were reproducible to within 15 mV. The differential absorption spectrum of the acridinyl radical was recorded by spectroelectrochemical reduction using a fixed potential of  $-0.7$  V vs SCE. The solution was deoxygenated and subjected to exhaustive reduction, with absorption spectra being recorded at frequent intervals. A similar experimental protocol was used to generate the differential absorption spectrum for the one-electron reduced species from methyl viologen in deoxygenated acetonitrile.

## Results and Discussion

**Spectroscopic Studies.** The 10-methylacridinium ion (**Acr**<sup>+</sup>) exhibits highly structured fluorescence in fluid solution that is characterized by a Stokes shift of ca. 30 nm in acetonitrile. The fluorescence quantum yield ( $\Phi_F$ ) is approximately 1.0, while the excited singlet state lifetime ( $\tau_S$ ) is  $31 \pm 2$  ns in the absence of oxygen. Weak phosphorescence can be detected around 620 nm in an ethanol glass at 77 K after addition of iodomethane (10% v/v). The lifetime of the triplet state under these conditions is  $5.5 \pm 0.5$  ms. Several research groups have described<sup>7,22,23,35</sup> the photophysical properties of 9-aryl-substituted 10-methylacridinium ions and, in particular, Fukuzumi et al.<sup>16</sup> have reported spectroscopic data for 9-mesityl-10-methylacridinium perchlorate at room temperature. We now describe the outcome of an independent investigation of the photophysical properties of this latter cation in order to properly establish a detailed understanding of the excited-state hierarchy. We have used the hexafluorophosphate salt for reasons of safety and improved solubility, but parallel studies were made with the perchlorate salt to ensure the absence of specific counterion effects.<sup>25</sup> In all cases, the results obtained for the two salts were indistinguishable. An X-ray crystal structural determination made for the perchlorate salt proved the authenticity of the compound, while the close comparability of the 500 MHz <sup>1</sup>H NMR spectra was taken as evidence that the hexafluorophosphate salt was of the appropriate purity.

The absorption spectrum recorded for **Mes-Acr**<sup>+</sup> in acetonitrile solution closely resembles that found for **Acr**<sup>+</sup>, indicating the dominant chromophore is the acridinium ion.<sup>35</sup> Fluorescence is observed under these conditions, but the spectrum differs markedly from that characteristic of **Acr**<sup>+</sup> (Figure 1). In deoxygenated acetonitrile,  $\Phi_F$  is only  $0.035 \pm 0.004$  while  $\tau_S$  is  $6.0 \pm 0.1$  ns. Decay of the excited state is monoexponential at all monitoring wavelengths and, in particular, contains no

(33) Oliveros, E.; Bossman, S. H.; Nonell, S.; Marti, C.; Heit, G.; Troscher, G.; Neuner, A.; Martinez, G.; Braun, A. M. *New J. Chem.* **1999**, 23, 85.

(34) (a) Branchi, B.; Bietti, M.; Ercolani, G.; Izquierdo, M. A.; Mitanda, M. A.; Stella, L. *J. Org. Chem.* **2004**, 69, 8874. (b) Jayanthi, S. S.; Ramamurthy, P. *J. Phys. Chem. A* **1997**, 101, 2016. (c) Sehested, K.; Holcman, J.; Hart, E. J. *J. Phys. Chem.* **1977**, 81, 1363. (d) Hubig, S. M.; Kochi, J. K. *J. Am. Chem. Soc.* **2000**, 122, 8279. (e) Bartl, J.; Steenken, S.; Mayr, H.; McClelland, R. A. *J. Am. Chem. Soc.* **1990**, 112, 6918.

(35) (a) Jonker, S. A.; Ariese, F.; Verhoeven, J. W. *Recl. Trav. Chim. Pays-Bas* **1989**, 108, 109. (b) Jonker, S. A.; van Dijk, S. I.; Goubitz, K.; Reiss, C. A.; Schuddeboom, W.; Verhoeven, J. W. *Mol. Cryst. Liq. Cryst.* **1990**, 183, 273. (c) Acheson, R. M., Ed. *Acridines*, 2nd ed.; Interscience Publishers: New York, 1973; Chapter 11.

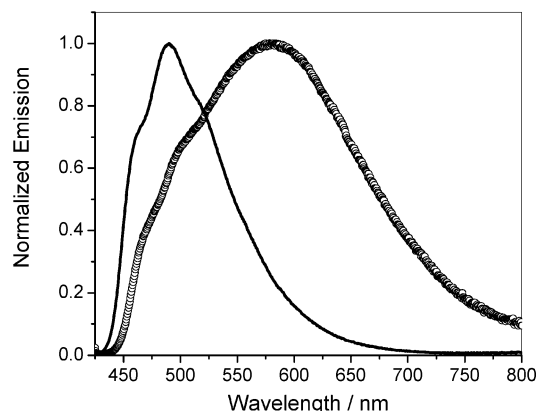


**Figure 1.** Normalized fluorescence spectra recorded for  $\text{Acr}^+$  (solid curve) and  $\text{Mes-Acr}^+$  (broken curve) in deoxygenated acetonitrile at room temperature.

contribution from a long-lived component. The corrected excitation spectrum is in excellent agreement with the absorption spectrum between 230 and 470 nm. Close examination of the fluorescence spectrum, however, reveals the existence of some fine structure on the high-energy side of the profile that coincides with the structured emission typical for the acridinium chromophore, while the low-energy side shows broad and unstructured emission similar to that reported for certain 9-aryl-10-methylacridinium ions with an electron-donating aryl group (Figure 1).<sup>7,22,23</sup> In these latter cases, fluorescence was attributed to a charge-transfer (CT) state in which the aryl group acts as donor and the acridinium ion as acceptor. The spectrum observed for  $\text{Mes-Acr}^+$  could be interpreted, therefore, as a mixture of fluorescence both from a locally excited (LE), acridinium-like singlet state and a CT state. It should be stressed that repeated purification of the sample had no effect on the fluorescence profile or lifetime.<sup>36</sup> Identical results were obtained for the perchlorate salt.

On exposure to subpicosecond laser pulses delivered at 430 nm the  $\text{S}_1\text{--S}_n$  transient absorption spectrum, which has a maximum at 470 nm, can be observed (Figure 2a). This spectrum shows pronounced absorption in the blue region but very little absorption at longer wavelengths. Over a period of 5 ps, the signal assigned to the LE singlet state evolves into a new absorption profile characterized by an absorption maximum around 500 nm and a pronounced shoulder at 550 nm (Figure 2b). This latter signal persists into the nanosecond time regime and is assigned to the singlet CT state. The strong absorption band around 500 nm can be attributed to the acridinyl radical,<sup>17</sup> while the mesityl radical cation is known to absorb around 470 nm.<sup>34d</sup> Neither species is expected to display significant absorption at 550 nm; the same situation is observed for 9-(1-naphthyl)-10-methylacridinium where there is an additional absorption transition superimposed over bands expected for the naphthyl radical cation and the acridinyl radical.<sup>7</sup> Given the close proximity and high redox power of the reactants, the 550 nm absorption band might be considered characteristic of strong electronic coupling within the CT state.

Formation of the singlet CT state occurs by way of first-order kinetics with a rise time of  $5 \pm 1$  ps in acetonitrile at room temperature (Figure 3a), in good agreement with the value reported by Fukuzumi et al.<sup>16</sup> Thus, the LE singlet state is heavily quenched compared to  $\text{Acr}^+$ , and the rate constant for intramolecular charge transfer ( $k_{\text{CT}}$ ) can be taken as ca.  $2 \times$

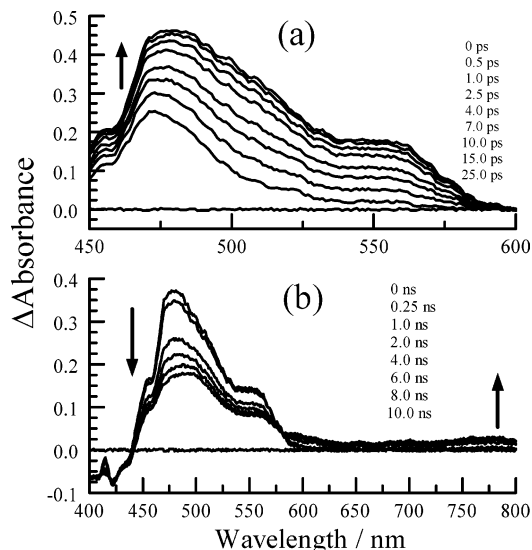


**Figure 2.** Transient differential absorption spectra recorded after laser excitation of  $\text{Mes-Acr}^+$  in acetonitrile at room temperature. (a) Excitation at 430 nm with a 0.2-ps laser pulse. (b) Excitation at 440 nm with a 20-ps laser pulse. Note the isosbestic points and the absorbance rise in the near-IR in panel b. The delay times are indicated on each panel.

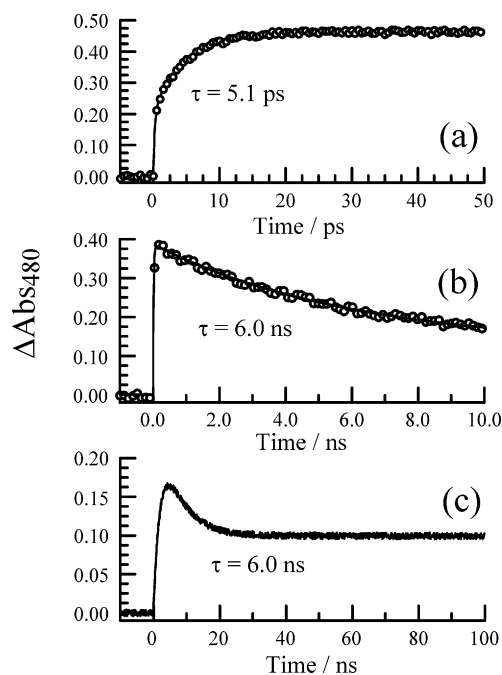


**Figure 3.** Kinetic traces recorded at 480 nm following laser excitation of  $\text{Mes-Acr}^+$  in acetonitrile at room temperature. (a) Excitation at 430 nm with a 0.2-ps laser pulse. (b) Excitation at 440 nm with a 20-ps laser pulse. (c) Excitation at 440 nm with a 20-ps laser pulse and with detection provided by a fast response digitizer.

$10^{11} \text{ s}^{-1}$ . This latter value is in good agreement with the lifetime of the LE state ( $\tau_{\text{LE}}$ ) of  $4.4 \pm 0.9$  ps derived by fluorescence upconversion spectroscopy. On this basis, we would expect to see much less LE fluorescence than is apparent in the spectrum recorded in acetonitrile.<sup>37</sup> In fact, a crude estimate based on deconvolution of the entire spectrum into LE and CT fluores-

(36) The compound was subjected to repeated column chromatography, TLC and recrystallization in an effort to minimize the contribution made by the LE fluorescence. Simultaneous analysis was made by time-resolved fluorescence to ensure the absence of a long-lived component in the decay records.

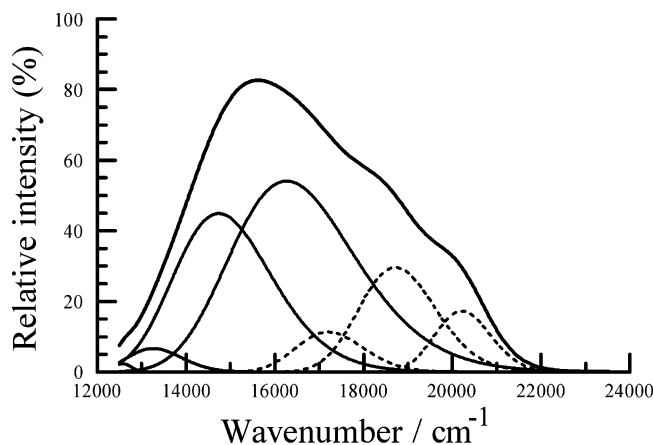


**Figure 4.** Deconvolution of the fluorescence spectrum recorded for **Mes-Acr<sup>+</sup>** in acetonitrile at room temperature into a series of Gaussian-shaped components. The three dashed curves are attributed to LE fluorescence, while the solid curves are assigned to fluorescence from the CT state. Note the fourth CT band cannot be properly resolved on this wavenumber range.

cence (Figure 4) indicates that the LE fluorescence contributes ca. 13% toward the total emission under these conditions.<sup>38</sup> Lifetime measurements eliminate the possibility that this residual LE fluorescence arises from an impurity. Even so, the derived  $k_{CT}$  value, taken together with the radiative rate constant measured for **Acr<sup>+</sup>** ( $k_{RAD} = 3 \times 10^7 \text{ s}^{-1}$ ), implies that the LE state should contribute only ca. 0.5% to the overall fluorescence profile under these conditions. The observed fluorescence spectrum can be reconstituted as a mixture of LE and CT states in which the population of the LE state is 2.5%. On this basis, it is considered that at room temperature virtually all of the observed LE fluorescence arises from thermal repopulation from the lower-energy CT state.<sup>39</sup> The relative population of LE and CT states corresponds to an energy gap of ca.  $9 \text{ kJ mol}^{-1}$  such that the rate constant for repopulation of the LE state would be ca.  $5 \times 10^9 \text{ s}^{-1}$ . The two states should now decay with a common lifetime of 6 ns,<sup>40</sup> as is observed at ambient temperature.

Further support was obtained for the concept of rapid thermal equilibration between LE and CT singlet states at and above room temperature via a temperature dependence study made in highly purified benzonitrile. With increasing temperature over the range of 20–130 °C the amount of structured fluorescence increases progressively, while there is a corresponding decrease in the unstructured fluorescence profile attributed to the CT state (Figure 5).<sup>41</sup> The relative ratio, after correction for the radiative

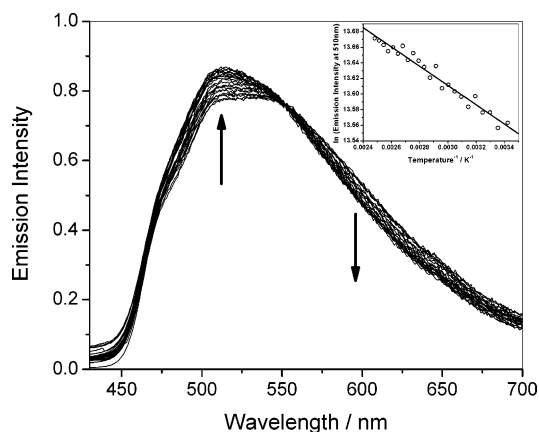


**Figure 5.** Effect of heating from 20 to 130 °C on the fluorescence spectrum of **Mes-Acr<sup>+</sup>** recorded in deoxygenated benzonitrile. The inset shows a plot to the Boltzmann expression.

rate constants of LE and CT states, can be well described in terms of the Boltzmann expression with an energy gap of  $8 \pm 1 \text{ kJ mol}^{-1}$ . This value is comparable to that estimated for **Mes-Acr<sup>+</sup>** in acetonitrile solution by deconvolution of the fluorescence spectrum and provides clear evidence that the LE and CT states reside in thermal equilibrium. The same situation arises in other solvents at ambient temperature, and the total fluorescence spectral profile can be split into contributions from LE and CT states. In all solvents, the amount of LE fluorescence exceeds that expected on the basis of its spontaneous lifetime. The results are easily explained, however, in terms of thermal equilibration between LE and CT singlet states. The energy gap remains around  $8\text{--}11 \text{ kJ mol}^{-1}$  in all solvents. It should be stressed that **Mes-Acr<sup>+</sup>** fluorescence does not follow Lippert–Mataga behavior,<sup>42</sup> presumably because there is no significant change in dipole moment upon excitation.

In propylene carbonate, the fluorescence properties remain similar to those described for acetonitrile with  $\Phi_F = 0.035$  and  $\tau_S = 5.1 \text{ ns}$  at 20 °C. However, on detection at the high-energy side, where the contribution of CT fluorescence is minimal, a short component could be picked up with a decay time of  $5 \pm 1 \text{ ps}$ . This coincides very well with the rate of formation of the CT state from the LE state as detected by ultrafast transient absorption spectroscopy under identical conditions. On cooling the solution, the contribution of this short component increases while, at the same time, in the continuous emission spectrum the contribution of LE fluorescence increases progressively. As such, the total fluorescence intensity also increases with decreasing temperature (Figure 6). The temperature dependence of the decay time of the short component, which corresponds to the rate constant ( $k_{LE}$ ) for conversion of LE to CT states, follows Arrhenius-type behavior in liquid solution with an

(37) The contribution made by LE fluorescence is somewhat solvent dependent and is notably higher in ethanol solution and a KBr disc. This is not a consequence of impurities since separate studies confirmed that our time-resolved fluorescence setup can easily resolve components due to **Mes-Acr<sup>+</sup>** and **Acr<sup>+</sup>** in mixtures, even when the latter is present at very low concentration.

(38) The fluorescence spectrum of **Acr<sup>+</sup>** was used as a reference system. This spectral profile was shifted to match that of the high-energy component observed for **Mes-Acr<sup>+</sup>**, and it was assumed, on the basis of Gaussian analyses, that the CT fluorescence is negligible at 510 nm. The CT “pure” fluorescence spectrum was compiled from the Gaussian bands and the two resolved spectra combined to give the best least-squares match to the observed spectrum.

(39) (a) Wasielewski, M. R.; Johnson, D. G.; Svec, W. A.; Kersey, K. M.; Minsek, D. W. *J. Am. Chem. Soc.* **1988**, *110*, 7219. (b) Heitele, H.; Frinckh, P.; Weeren, S.; Pollinger, F.; Michel-Beyerle, M. E. *J. Phys. Chem.* **1989**, *93*, 5173. (c) Harriman, A.; Heitz, V.; Ebersole, M.; van Willigen, H. *J. Phys. Chem.* **1994**, *98*, 4982.

(40) (a) Ford, W. E.; Rodgers, M. A. J. *J. Phys. Chem.* **1992**, *96*, 2917. (b) Hissler, M.; Harriman, A.; Khatyr, A.; Ziessel, R. *Chem. Eur. J.* **1999**, *5*, 3366.

(41) (a) It should be noted that the apparent fluorescence maximum differs in acetonitrile ( $\lambda \approx 590 \text{ nm}$ ), benzonitrile ( $\lambda \approx 560 \text{ nm}$ ), and propylene carbonate ( $\lambda \approx 570 \text{ nm}$ ) as shown in Figures 1, 5, and 6. This is due to very slight changes in the equilibrium distribution of LE and CT states in the different solvents. Because of the vastly different radiative rates, a trivial increase in the percentage of the LE state moves the emission maximum towards the blue. Detailed spectral curve fitting shows that the solvent has minimal effect on the actual energy levels of these two states. The equilibrium distribution is also changed slightly on addition of electrolytes such as tetra-*N*-butylammonium hexafluorophosphate. Such effects have been reported earlier for related 9-aryl-10-methylacridinium salts, see: (b) Horng, M. L.; Dahl, K.; Jones, G., II; Maroncelli, M. *Chem. Phys. Lett.* **1999**, *315*, 363.

(42) (a) Lippert, E. Z. *Naturforsch.* **1955**, *10a*, 541. (b) Mataga, N.; Kaifu, Y.; Koizumi, M. *Bull. Chem. Soc. Jpn.* **1955**, *28*, 690.



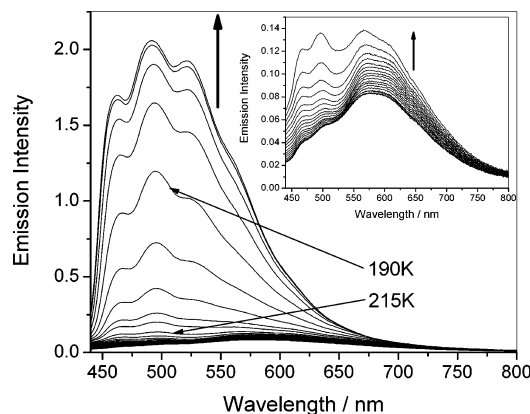


**Figure 6.** Effect of cooling from 300 to 130 K on the fluorescence spectrum recorded for **Mes-Acr**<sup>+</sup> in propylene carbonate. The inset shows an expansion of the ambient temperature region so as to better reveal the CT fluorescence, with spectra run each 5 K. Low-temperature spectra refer to 130, 140, 150, and 160 K.

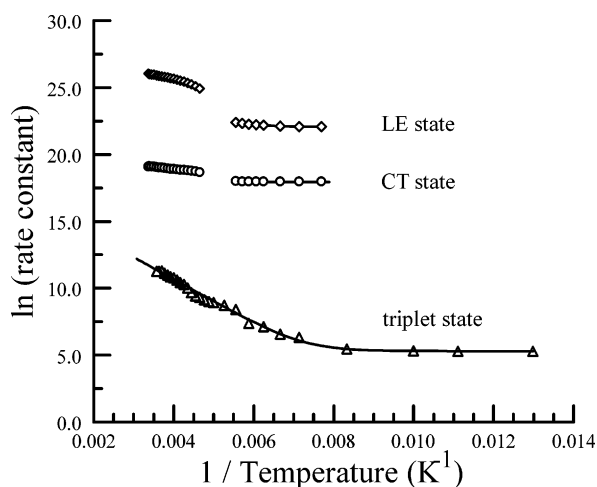


**Figure 7.** Arrhenius-type plots constructed for the different processes observed for **Mes-Acr**<sup>+</sup>. The data points refer to LE (◇) and CT (○) fluorescence in fluid and glassy propylene carbonate while the solid lines are least-squares fits as described in the text. The remaining data set refers to the triplet excited state (△) in butyronitrile, as measured by transient absorption spectroscopy. The gap in the time-resolved fluorescence data sets corresponds to the phase transition of the solvent, and the derived rate constants do not follow a continuous curve over this region.

activation energy ( $E_A$ ) of  $6.5 \text{ kJ mol}^{-1}$  and a preexponential factor ( $\nu = 2.8 \times 10^{12} \text{ s}^{-1}$ ) that approaches the vibrational limit. In a glassy matrix,  $k_{LE}$  remains activated and fits better to the modified Arrhenius expression given as eq 1

$$k = k_0 + k_1 \exp\left(-\frac{\Delta E_1}{RT}\right) \quad (1)$$

(Figure 7). Here, the activationless rate constant ( $k_0$ ) has a value of  $3.6 \times 10^9 \text{ s}^{-1}$ , while the activated parameters  $k_1$  and  $\Delta E_1$  have values of  $4 \times 10^{11} \text{ s}^{-1}$  and  $12 \text{ kJ mol}^{-1}$ , respectively. It is important to note that even at the lowest temperature attained ( $T = 130 \text{ K}$ ) conversion of LE to CT dominates over radiative decay from the LE state. This is evidenced by the fact that the prompt fluorescence lifetime ( $\tau_{LE} = 0.27 \text{ ns}$ ) is very much reduced relative to that of **Acr**<sup>+</sup> ( $\tau_s = 31 \text{ ns}$ ), while the total fluorescence spectrum contains important contributions from both CT and LE states. The energy gap between these two states is reduced somewhat at low temperature.

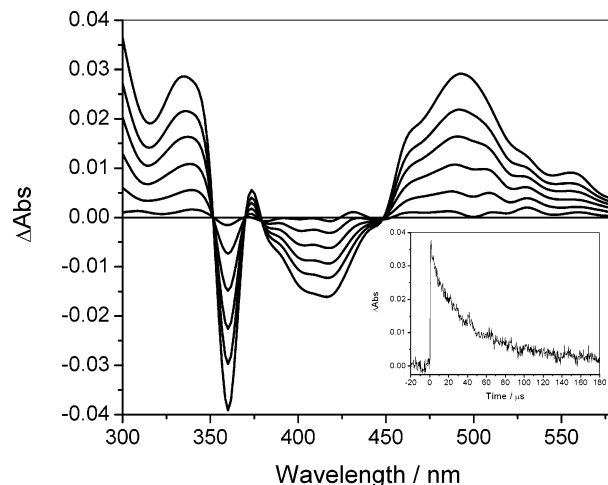


**Figure 8.** Microsecond triplet–triplet differential absorption spectra recorded at different times after laser excitation of **Mes-Acr**<sup>+</sup> in deoxygenated acetonitrile with a 4-ns laser pulse at 355 nm. The inset shows a kinetic trace recorded at 480 nm at very low laser power. The individual spectra were recorded at delay times of 11, 20, 27, 40, 60, and  $100 \mu\text{s}$  and show the progressive recovery of the ground state.

Detection at low energy ( $\lambda = 600 \text{ nm}$ ), where the CT fluorescence makes the dominant contribution, allows study of the temperature dependence of the processes by which the CT state decays ( $k_{CT}$ ). It should be stipulated that  $k_{CT}$  is the sum of at least three rate constants; namely, thermal repopulation of LE ( $k_{LE}$ ), internal conversion to the ground state, and intersystem crossing to the triplet manifold. In fluid solution, the temperature dependence of  $k_{CT}$  follows Arrhenius behavior with  $E_A = 2.8 \text{ kJ mol}^{-1}$  and an apparent preexponential factor ( $\nu$ ) of  $6 \times 10^8 \text{ s}^{-1}$  (Figure 7). The decay rate constant ( $k_{CT} \approx 6 \times 10^7 \text{ s}^{-1}$ ) becomes activationless well below the glass transition temperature. It is important to note that the dynamics of the CT state vary only over a rather restricted range and that its lifetime remains in the nanosecond domain even at the lowest temperature attained ( $\tau_{CT} = 18.6 \text{ ns}$  at  $130 \text{ K}$ ) in sharp contrast to the strong temperature dependence and lifetime of several hours at low temperature reported by Fukuzumi et al., admittedly in a different solvent.<sup>16</sup> We find no obvious solvent dependence for this process and no effect of the counterion. In fact, the very weak temperature dependence of  $k_{CT}$  observed here is quite typical of electron-transfer processes involving a large energy gap (i.e., inverted region conditions) where nuclear tunneling<sup>6</sup> and other quantum chemical effects<sup>5</sup> allow the process to avoid the high activation barrier expected on the basis of a fully classical description.<sup>3</sup>

The transient absorption studies indicate that the CT state decays with a lifetime of  $6 \pm 1 \text{ ns}$  (Figure 3b), in excellent agreement with the time-resolved fluorescence spectral data, to leave a residual transient signal (Figure 3c). Investigation of the long-lived species by excitation of **Mes-Acr**<sup>+</sup> in deoxygenated acetonitrile with a 4-ns laser pulse and observation into the microsecond domain gives rise to a transient spectrum that shows bleaching around 350–450 nm and absorption in the range of 450–600 nm (Figure 8). This spectrum is similar, but not identical, to that observed at the end of the picosecond laser flash photolysis records (Figure 9a). The transient decays via first-order kinetics over a wide variation in laser power, but there are indications for a second-order component at very high intensities. The globally averaged lifetime is  $30 \pm 5 \mu\text{s}$  under

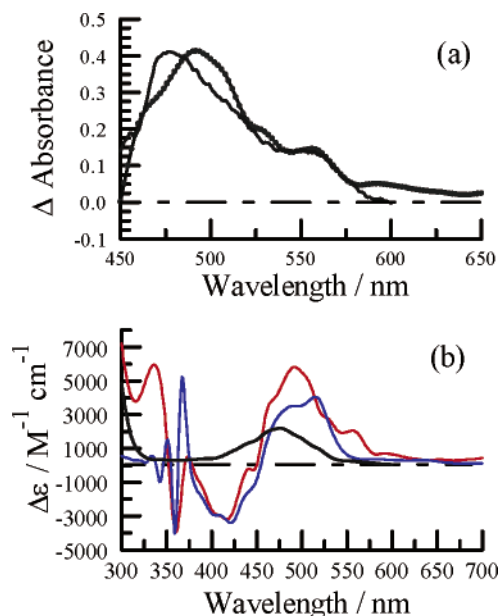


**Figure 9.** (a) Comparison of differential transient absorption spectra recorded for the CT (solid line) and triplet (●) states of **Mes-Acr**<sup>+</sup> in deoxygenated acetonitrile at 20 °C. (b) Comparison of the differential absorption spectra recorded for the triplet state (red), the acridinyl radical (blue), and the mesityl  $\pi$ -radical cation (black) in deoxygenated acetonitrile.

these conditions. This species is formed with a quantum yield of  $0.38 \pm 0.06$ . The quantum yield is increased a factor of 2.3-fold on addition of iodomethane (10% v/v), where the lifetime decreases to  $700 \pm 50$  ns. Given that this species evolves from the singlet CT state, and taking account of the effect of iodomethane, it can be identified as being either a triplet CT state or a locally excited triplet state. It should be noted that the transient signal decays cleanly to the prepulse baseline and that the spectral changes involve several isosbestic points. These findings are taken to suggest that only one species is involved.

The transient differential absorption spectrum observed on the microsecond time scale is similar to that reported by Fukuzumi et al.,<sup>16</sup> although their assignment as the singlet CT state cannot be correct since this latter species has a lifetime of only 6 ns. In any case, the spectrum differs from that observed on subnanosecond time scales and that is clearly assignable to the singlet CT state. The longer-lived spectral profile is remarkably similar to that assigned to the LE triplet state of certain aryl-substituted 10-methylacridinium ions,<sup>22,35</sup> and in particular there is close agreement with the spectrum of the triplet state observed for 9-phenyl-10-methylacridinium (see the Supporting Information). While it bears resemblance to the differential spectrum observed for the **Mes-Acr**<sup>+</sup> acridinyl radical produced by spectroelectrochemistry,<sup>17</sup> there are important discrepancies (Figure 9b). The most obvious difference is that the sharp absorption peak seen at 370 nm for the radical is absent from the spectrum recorded for the 30- $\mu$ s transient, while only the latter transient shows a strong absorption peak around 330 nm. Furthermore, the difference between these two spectra does not match the known absorption spectrum of the mesityl  $\pi$ -radical cation, which absorbs weakly around 475 nm (Figure 9b).<sup>34</sup> The 30- $\mu$ s transient absorption persists into the far-red region (see Figure 2b), showing weak absorbance as far as 750 nm, where the acridinyl radical is transparent. Consequently, the transient species is most likely the LE triplet state arising from intersystem crossing. In this respect, it is important to note

that phosphorescence from **Mes-Acr**<sup>+</sup> has been observed in an ethanol glass at 77 K.<sup>17,43</sup>

The transient absorption signal now attributed to the locally excited triplet state of **Mes-Acr**<sup>+</sup> was quenched by molecular oxygen in acetonitrile with a bimolecular rate constant of  $2.0 \pm 0.3 \times 10^9 \text{ M}^{-1} \text{ s}^{-1}$ . This value is close to the one-ninth diffusion controlled limit usually observed for O<sub>2</sub> quenching of a local triplet state. At all concentrations of dissolved O<sub>2</sub>, the signal decayed to the prepulse baseline without leaving a longer-lived species assignable to the mesityl  $\pi$ -radical cation.<sup>36</sup> Instead, quenching resulted in the formation of singlet molecular oxygen with a quantum yield of  $0.42 \pm 0.05$ . The so-formed singlet molecular oxygen decayed via first-order kinetics with a lifetime of  $60 \pm 5 \mu\text{s}$ . The perchlorate salt behaved identically.<sup>44</sup>

Fukuzumi et al.<sup>16</sup> have reported that the long-lived transient, identified here as being the local triplet state, decays via a strongly activated process. Indeed, their activation energy as recalculated from the quoted reorganization energy and driving force is  $7.0 \text{ kJ mol}^{-1}$  in benzonitrile solution. According to the energy-gap law,<sup>45</sup> nonradiative decay of a local triplet state is not expected to show a significant temperature dependence, but it is not unusual for CT states to decay by way of activated routes. It was observed that the lifetime of triplet **Mes-Acr**<sup>+</sup> in butyronitrile increased with decreasing temperature over the range  $300 < T < 140 \text{ K}$  but became essentially temperature independent at lower temperatures (Figure 7). At 77 K, both transient absorption spectroscopy and time-resolved phosphorescence indicated that the triplet lifetime was  $5 \pm 2 \text{ ms}$ . Overall, the kinetic data give a reasonable fit to eq 1 with  $k_0 = 200 \text{ s}^{-1}$ ,  $k_1 = 3.2 \times 10^7 \text{ s}^{-1}$ , and  $\Delta E_1 = 13.8 \text{ kJ mol}^{-1}$ . This analysis shows that the triplet state decays by both activated and activationless processes.<sup>46</sup> The latter step is most likely associated with nonradiative decay through vibrational modes and will be controlled by the energy-gap law. The activated route is more difficult to rationalize but does not refer to thermal repopulation of singlet or triplet CT states since the derived energy barrier ( $\Delta E_1 = 13.8 \text{ kJ mol}^{-1}$ ) is significantly less than the spectroscopic energy gap ( $\Delta E = 60 \text{ kJ mol}^{-1}$ ) between these states. It is more likely that the activated process is associated with a conformational change accessible to the triplet state. As such, it is important to note that the 9-phenyl-10-methylacridinium ion shows similar behavior although intramolecular charge transfer does not take place in this molecule.<sup>47</sup>

**Energy Levels.** An important aspect of this investigation relates to the accurate positioning of the various excited-state

(43) The phosphorescence signal, which decays with a lifetime of 5.3 ms, is enhanced a factor of 2.5-fold upon addition of iodomethane (10% v/v). Under these latter conditions, the lifetime decreases to 3.3 ms. The phosphorescence spectrum is comparable to that observed for **Acr**<sup>+</sup> under identical conditions, except for a small red shift.

(44) Illumination of **Mes-Acr**<sup>+</sup> in O<sub>2</sub>-saturated acetonitrile has been reported previously but only in the presence of 9,10-dimethylanthracene (ref 20), where electron transfer might compete with singlet oxygen formation. In view of the high quantum yield for singlet oxygen production found here, together with the reinterpretation of the long-lived intermediate species, the mechanism given for the photooxygenation of anthracene derivatives needs to be reconsidered.

(45) Englman, R.; Jortner, J. *Mol. Phys.* **1970**, *18*, 145.

(46) The activated process observed at higher temperatures is not too dissimilar from that reported by Fukuzumi et al. (ref 16), allowing for the different solvents, although the derived parameters are different. The real disparity, however, is that whereas our results indicate the onset of an activationless process at low temperature, Fukuzumi et al. (ref 16) reported Arrhenius-type behavior even in frozen media. We have shown previously (ref 17) that the low-temperature EPR results are better explained in terms of a sacrificial photoreaction involving amine impurities in the solvent.



energy levels. The energy of the LE singlet state can be identified as the intersection between fluorescence and excitation spectra recorded in a glassy matrix at 77 K. This provides a precise energy for the LE state of  $2.70 \pm 0.02$  eV. An estimate of the same energy gap in acetonitrile at room temperature, as obtained from an overlap of normalized absorption and fluorescence spectra after deconvolution into Gaussian components, is  $2.67 \pm 0.03$  eV. Fukuzumi et al.<sup>16</sup> calculated the energy of the CT state from electrochemical potentials measured in acetonitrile, but this approach is likely to underestimate the energy gap because of the irreversible nature of the mesityl oxidation peak.<sup>48</sup> A more reliable procedure involves analysis of the reduced charge-transfer fluorescence spectrum recorded in acetonitrile at room temperature.<sup>26</sup> For this purpose, the reduced fluorescence spectrum was deconvoluted into the minimum number of Gaussian components and interpreted as a mixture of LE and CT fluorescence bands (Figure 4). The latter bands are easily identified by their relative broadness. Four peaks are needed to fully fit the entire CT fluorescence profile recorded under these conditions. The averaged separation between these peaks of  $1450\text{ cm}^{-1}$  can be assigned to a vibrational bending mode that is coupled to deactivation of the excited state. The highest energy CT fluorescence peak ( $E_{00}$ ) is centered at  $18\,400\text{ cm}^{-1}$ . The full width at half-maximum of each Gaussian component increases with increasing temperature and corresponds to a reorganization energy ( $\lambda_{CT}$ ) of  $0.29 \pm 0.02$  eV. The latter term is somewhat solvent dependent, decreasing to 0.23 eV in butyronitrile and decreasing further to 0.14 eV in octanitrile. Moreover, the sum of  $E_{00}$  and  $\lambda_{CT}$  corresponds to the energy of the CT state in acetonitrile solution;<sup>49</sup> the derived value is  $2.57 \pm 0.04$  eV. As expected, this latter value is significantly higher than that estimated by electrochemical methods ( $E_{CT} = 2.37$  eV).<sup>16</sup> It is also important to note that the reorganization energy determined from spectral curve fitting is markedly lower than that reported ( $\lambda_{CT} = 0.79$  eV) by Fukuzumi et al.<sup>16</sup> on the basis of an Arrhenius-type plot. A crude estimate of the reorganization energy ( $\lambda_{LE}$ ) associated with population of the LE state, taken as half the relevant Stokes shift, is 0.04 eV in acetonitrile.<sup>50</sup> Comparable values were derived for **Mes-Acr**<sup>+</sup> in a range of solvents of varying polarity.

From low-temperature phosphorescence spectra, the triplet energy ( $E_T$ ) of **Mes-Acr**<sup>+</sup> is calculated to be  $1.94 \pm 0.03$  eV. A similar value was observed for **Acr**<sup>+</sup> ( $E_T = 2.00$  eV) and for several related 9-aryl-10-methylacridinium ions ( $E_T \approx 1.9$ ).<sup>22</sup> It is likely, therefore, that each triplet state in these ions is localized on the acridinium nucleus. This analysis places the triplet state of **Mes-Acr**<sup>+</sup> some 0.63 eV below the singlet CT state; a similar situation was reported previously for the 9-(1-naphthyl)-10-methylacridinium ion.<sup>7</sup> Fukuzumi et al.<sup>16</sup> have reported that the CT state of **Mes-Acr**<sup>+</sup> oxidizes anthracene in deaerated acetonitrile solution. We have confirmed that irradiation

of **Mes-Acr**<sup>+</sup> in acetonitrile in the presence of anthracene (0.2–5 mM) with a 4-ns laser pulse at 430 nm leads to the production of the anthracene radical cation and the corresponding acridinyl radical. The bimolecular rate constant for this process is ca.  $2.0 \times 10^9\text{ M}^{-1}\text{ s}^{-1}$ . Taking account that the CT state has a lifetime of only 6 ns under these conditions,<sup>51</sup> it seems more likely that electron transfer occurs to the triplet state of **Mes-Acr**<sup>+</sup>. Indeed, the reduction potential for the triplet state, calculated from the reversible reduction potential ( $E_{RED} = -0.49\text{ V vs SCE}$ )<sup>17</sup> and the triplet energy ( $E_T = 1.94\text{ eV}$ ), is  $+1.45\text{ V vs SCE}$ . As such, oxidation of anthracene ( $E_{OX} = +1.09\text{ V vs SCE}$ )<sup>52</sup> by the triplet state is thermodynamically favorable ( $\Delta G^0 = -0.36\text{ eV}$ ).<sup>53</sup> Related studies has confirmed that the triplet state of 9-(1-naphthyl)-10-methylacridinium also oxidizes anthracene under these conditions with a bimolecular rate constant of ca.  $1.5 \times 10^9\text{ M}^{-1}\text{ s}^{-1}$ .<sup>7</sup>

On the basis of the derived energy levels, the **Mes-Acr**<sup>+</sup> triplet state is not expected to reduce electron acceptors even as strong as methyl viologen (**MV**<sup>2+</sup>) in polar solution since the thermodynamic driving force is highly unfavorable ( $\Delta G^0 > +40\text{ kJ mol}^{-1}$ ). Surprisingly, it was observed that steady-state illumination ( $\lambda > 350\text{ nm}$ ) of **Mes-Acr**<sup>+</sup> in deoxygenated acetonitrile containing **MV**<sup>2+</sup> (5 mM) resulted in the appearance of the characteristic blue color associated with reduced viologen (**MV**<sup>•+</sup>). Although formed in very low concentration, **MV**<sup>•+</sup> was found to persist in solution for many minutes unless molecular oxygen was present. In fact, **MV**<sup>•+</sup> accumulates quickly but once a steady-state concentration is reached further illumination has no effect. The blue coloration does not develop if a few drops of concentrated acid are added prior to illumination.

Control studies showed that **MV**<sup>2+</sup> did not quench fluorescence from the CT state ( $k_Q < 4 \times 10^8\text{ M}^{-1}\text{ s}^{-1}$ ) or the triplet lifetime ( $k_Q < 5 \times 10^5\text{ M}^{-1}\text{ s}^{-1}$ ) in deoxygenated acetonitrile.<sup>54</sup> Even so, laser excitation of **Mes-Acr**<sup>+</sup> in deoxygenated acetonitrile in the presence of **MV**<sup>2+</sup> resulted in formation of **MV**<sup>•+</sup> as evidenced from transient absorption spectroscopy. It was observed that, whereas the rate of formation of **MV**<sup>•+</sup> increased linearly with increasing **MV**<sup>2+</sup> concentration, corresponding to a bimolecular rate constant of  $1.3 \times 10^7\text{ M}^{-1}\text{ s}^{-1}$ , the yield of **MV**<sup>•+</sup> reached a maximum value and did not increase with further addition of **MV**<sup>2+</sup>. The optimized quantum yield for formation of **MV**<sup>•+</sup>, calculated by comparison to the triplet state at high **MV**<sup>2+</sup> concentration, was only  $0.05 \pm 0.01$ . Extensive purification of the solvent led to a progressive decrease in the yield of reduced viologen. All indications point to the appearance of **MV**<sup>•+</sup> as arising from a minor sacrificial side-reaction perhaps associated with the high instability of the mesityl  $\pi$ -radical cation. This species deprotonates, even in acidic solution, and reacts rapidly with nucleophiles.<sup>34c</sup>

(47) For 9-phenyl-10-methylacridinium hexafluorophosphate, which does not show an intramolecular CT state, the local triplet state decays via first-order kinetics with  $\tau_T = 10\text{ }\mu\text{s}$  in deoxygenated  $\text{CH}_2\text{Cl}_2$  at room temperature (ref 22). The phosphorescence lifetime recorded at 77 K in ethanol containing 10% v/v iodomethane is 4 ms.

(48) (a) The reduction potential for one-electron oxidation of mesitylene in acetonitrile is reported as 1.88 V (ref 48b) vs SCE or 2.1 V (ref 48c) vs SCE. In our hands, the oxidative peak is highly irreversible due to a following chemical process. (b) Fukuzumi, S.; Ohkubo, K.; Suenobu, T.; Kato, K.; Fujitsuka, M.; Ito, O. *J. Am. Chem. Soc.* **2001**, *123*, 8459. (c) Gould, I. R.; Moser, J. E.; Armitage, B.; Farid, S. *J. Am. Chem. Soc.* **1989**, *111*, 1917.

(49) Kjaer, A. M.; Ulstrup, J. *J. Am. Chem. Soc.* **1988**, *110*, 3874.

(50) Englman, R.; Jortner, J. *Mol. Phys.* **1970**, *18*, 145.

(51) At the highest concentration of anthracene used (5 mM) ca. 15% of the CT singlet state would be quenched, but triplet quenching would be quantitative.

(52) Baird, A.; Lund, H., Eds. *Encyclopedia of the Electrochemistry of the Elements. Organic Section*; Marcel Dekker: New York, 1984; Vol. XI.

(53) Given the relative triplet energies of **Mes-Acr**<sup>+</sup> ( $E_T = 1.94\text{ eV}$ ) and anthracene ( $E_T = 1.84\text{ eV}$ ), it might be argued that triplet energy transfer should compete with electron transfer from triplet **Mes-Acr**<sup>+</sup>. However, the resultant triplet excited state of anthracene is a good reductant and will reduce ground-state **Mes-Acr**<sup>+</sup> ( $\Delta G^0 = -0.26\text{ eV}$ ). The net effect, therefore, is the production of the anthracene  $\pi$ -radical cation by both routes.

(54) It should be noted that the triplet lifetime was lowered in the presence of reduced viologen that accumulates under exposure to repeated laser pulses. With the use of a flow cell and low repetition rate that allows the solution to be replenished for each laser shot it was shown conclusively that **MV**<sup>2+</sup> does not quench the triplet state under these conditions.

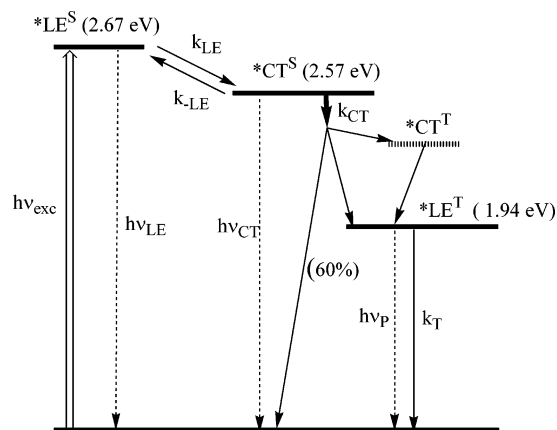


**Figure 10.** Energy level diagram proposed for **Mes-Acr<sup>+</sup>**. All the excited states indicated have been identified spectroscopically except for the triplet CT state (\*CT<sup>T</sup>). State energies are only weakly medium dependent; values indicated refer to acetonitrile solution for singlets and to ethanol at 77 K for the LE triplet. Solid arrows represent the major nonradiative decay pathways following excitation of the acridinium chromophore. In addition, dashed arrows represent the three (minor) radiative decay routes. The following terms apply to individual rate constants:  $k_{LE}$ , charge transfer from the LE singlet to form the CT state;  $k_{-LE}$ , reverse charge transfer to reform the LE singlet state;  $k_T$ , nonradiative decay of the LE triplet to reform the ground state.

We note that radiative decay from the CT state is inefficient, despite the relatively long lifetime of this state, and there is clear evidence for intersystem crossing to the triplet manifold. Earlier work<sup>22</sup> has considered two mechanisms for triplet formation in 9-aryl-10-methylacridinium ions. Thus, in a polar solvent at ambient temperature, a likely route to the locally excited triplet involves intersystem crossing within the CT state to form the corresponding triplet CT state. Reverse charge transfer within this latter species would result in population of the acridinium-like LE triplet state, provided this species lies at lower energy. The effect of iodomethane is to promote intersystem crossing between the CT states. Alternatively the LE triplet could arise directly from the singlet CT state via coupled electron transfer and spin inversion, a process enhanced by the spin–orbit coupling resulting from the nearly perpendicular orientation of the two units.<sup>55</sup> Spin polarization studies of systems closely related to **Mes-Acr<sup>+</sup>** have indicated that the latter mechanism dominates,<sup>22</sup> but later studies on other dyads involving (nearly) orthogonal donor and acceptor moieties showed the operation of both mechanisms.<sup>56</sup> At low temperatures, where formation of the CT state is incomplete, intersystem crossing from singlet LE to triplet LE could contribute, but because the triplet yield in **Acr<sup>+</sup>** is small this path is considered to be relatively unimportant. It is interesting to note that iodomethane enhances triplet formation by a factor of ca. 2.4-fold at both room temperature and 77 K. At room temperature, the LE triplet state is formed with a quantum yield of only 0.38. This means that direct internal conversion to the ground state must occur from the singlet CT state, and in view of the low CT fluorescence quantum yield this must be a nonradiative process.

On the basis of the above discussion, an energy level diagram can now be constructed for **Mes-Acr<sup>+</sup>** (Figure 10). Our spectral

analysis shows that the energy gap between LE and CT states is only ca. 0.1 eV. This close positioning of the energy levels accounts for the delayed fluorescence observed for the LE state in fluid solution, and it should be noted that the energy gaps obtained by spectral curve fitting and Boltzmann analyses of the continuous spectra are identical within experimental error. Solvent polarity has only a small effect on this energy gap, presumably because the process under investigation is charge shift, not charge separation/recombination.

Decay of the LE singlet state to the CT state is weakly activated in solution but approaches an activationless rate ( $k_{LE} = 3.6 \times 10^9 \text{ s}^{-1}$ ) in a glassy matrix. This latter process might refer to nuclear tunneling, which is known to be favored at low temperature.<sup>6</sup> The apparent activation energy ( $E_A = 6.5 \text{ kJ mol}^{-1}$ ) found in fluid propylene carbonate is close to that estimated ( $E_A \approx 5.4 \text{ kJ mol}^{-1}$ ) from classical Marcus theory,<sup>3</sup> while the limiting rate constant ( $k_{LE} \approx 3 \times 10^{12} \text{ s}^{-1}$ ) approaches the vibrational limit. In the event that charge transfer occurs within the framework of Marcus theory,<sup>3</sup> the electronic coupling matrix element can be calculated as being ca.  $75 \text{ cm}^{-1}$  at room temperature. This derived value might be considered rather high for charge transfer across an orthogonal geometry, but as noted above, the transient absorption spectrum of the CT state indicates that considerable electronic interaction between the two moieties occurs.

In propylene carbonate, decay of the CT state is activationless in the glass ( $k_{CT} = 6 \times 10^7 \text{ s}^{-1}$ ) and weakly activated ( $E_A = 2.5 \text{ kJ mol}^{-1}$ ;  $k_{CT} = 6 \times 10^8 \text{ s}^{-1}$ ) in fluid solution.<sup>57</sup> These derived  $k_{CT}$  values are considerably smaller than the vibrational limit ( $k \approx 10^{13} \text{ s}^{-1}$ ). It should be stressed that these activation parameters relate to a process that bifurcates from the CT state into a spin-forbidden process to the local triplet state (ca. 38%) and a spin-allowed process to the ground state ( $\geq 60\%$ ) (Figure 10). As such, the derived activation energy cannot be associated with a particular decay route.

## Concluding Remarks

Rapid charge transfer occurs within the LE singlet state of **Mes-Acr<sup>+</sup>** in fluid solution to generate the corresponding CT state. This latter species fluoresces, thereby allowing precise determination of its lifetime and energy, but decays mainly by way of nonradiative processes. The fluorescence differs markedly in profile and lifetime from that characterized for the LE singlet state... and this difference can be unambiguously assigned to a contribution of CT fluorescence.<sup>58</sup> Similar fluorescence properties have been observed for related 9-aryl-substituted acridinium ions in solution, but the energy levels of **Mes-Acr<sup>+</sup>** are such that the LE and CT states reside in thermal equilibrium at ambient temperature. The singlet CT state is sufficiently long-lived for this latter equilibrium to be established on the relevant time scale and, because of the small energy gap, the rate of repopulation of the LE state is relatively fast. It seems remarkable that these two charge-transfer processes occur on the subnanosecond time scale despite the fact that the mesityl

(55) Okada, T.; Karaki, I.; Matsuzawa, E.; Mataga, N.; Sakata, Y.; Misumi, S. *J. Phys. Chem.* **1981**, *85*, 3957.

(56) Wiederrecht, G. P.; Svec, W. A.; Wasielewski, M. R.; Galili, T.; Levanon, H. *J. Am. Chem. Soc.* **2000**, *122*, 9715.

(57) (a) The apparent temperature dependence in fluid solution can be traced to small changes in the energy gap, connected with frequency changes in solvent librations. This effect disappears in a glassy matrix. (b) Claude, J. P.; Meyer, T. J. *J. Phys. Chem.* **1995**, *99*, 51.

(58) Fukuzumi et al. (ref 16) report that the absorption and fluorescence spectra of **Mes-Acr<sup>+</sup>** are superpositions of the spectra of each component, that is mesitylene and **Acr<sup>+</sup>**. There is no mention of CT fluorescence, although this is well documented for related compounds (refs 22, 23, 34).

and acridinium subunits are held in an orthogonal geometry. Electronic coupling under such conditions might be expected to be at a minimum,<sup>59</sup> although the reactants are in close proximity and charge transfer can proceed along the connecting  $\sigma$ -bond. In fact, our analysis suggests that the coupling element is ca. 75 cm<sup>-1</sup>.

Once formed, the singlet state is deactivated primarily by way of nonradiative processes. Our quantitative studies indicate that the CT state contributes 97.5% to the equilibrium mixture of excited singlet states but that the LE triplet is formed with a yield of only 38%. Indeed, formation of the longest-lived transient species, regardless of its assignment, must be less than 43% to account for the observed effect of iodomethane.<sup>60</sup> For 9-(1-naphthyl)-10-methylacridinium, addition of iodomethane causes a 7-fold increase in the yield of the LE triplet state.<sup>7</sup> It is most likely that the singlet CT state partitions between charge transfer to reestablish the ground state (60%) and intersystem crossing (38%) (via a triplet CT state) to the lowest LE triplet,<sup>55</sup> which resides on the acridinium unit. The observation of long-lived phosphorescence from **Mes-Acr**<sup>+</sup>, **Acr**<sup>+</sup>, and 9-(1-naphthyl)-10-methylacridinium at 77 K provides clear evidence that the LE triplet lies at lower energy than the singlet CT state.

(59) Lappe, J.; Cave, R. J.; Newton, M. D.; Rostov, I. V. *J. Phys. Chem. B* **2005**, *109*, 6610.

(60) Fukuzumi et al. (ref 16) report this quantum yield as being 0.98, on the basis of a comparative method apparently using anthracene as quencher, but this value is inconsistent with the noted effect of iodomethane.

(61) Ohkubo, K.; Kotani, H.; Fukuzumi, S. *Chem. Commun.* **2005**, 4520.

Under the conditions where Fukuzumi et al.<sup>16</sup> report that the singlet CT state survives for some hours, namely frozen benzonitrile at 203 K, it is now apparent that the LE triplet will be the longest-lived species. This triplet has a lifetime of 5.3 ms at 77 K, in the absence of a sacrificial electron donor.<sup>17</sup> Formation of the local acridinium-based triplet with a microsecond lifetime was also confirmed by transient absorption spectroscopic studies (see the Supporting Information). Persistent discolorations reported to result from continuous irradiation at low temperature must be the result of photodecomposition.<sup>17,61</sup>

**Acknowledgment.** We thank the EPSRC (EP/C007721/1), the University of Amsterdam, and the University of Newcastle for financial support. All EPR studies were made at the EPSRC-supported EPR Centre at the University of Manchester. Singlet molecular oxygen measurements were made at the Free Radical Research Facility at the Daresbury Laboratory.

**Supporting Information Available:** Analytical data for the perchlorate salt of **Mes-Acr**<sup>+</sup>, including ES-MS, <sup>1</sup>H NMR, C/H/N analysis and X-ray structure, comparison of triplet absorption spectra for **Mes-Acr**<sup>+</sup> and 9-phenyl-10-methylacridinium, and the difference between transient differential absorption spectra recorded for the triplet and acridinyl radical, transient differential absorption spectrum recorded at 77 K. This material is available free of charge via the Internet at <http://pubs.acs.org>.

JA052967E